UNIVERSIDADE ESTADUAL DE CAMPINAS
SISTEMA DE BIBLIOTECAS DA UNICAMP
REPOSITÓRIO DA PRODUÇÃO CIENTIFICA E INTELECTUAL DA UNICAMP

Versão do arquivo anexado / Version of attached file:

Versão do Editor / Published Version

Mais informações no site da editora / Further information on publisher's website:

https://aip.scitation.org/doi/10.1063/1.4871807

DOI: 10.1063/1.4871807

Direitos autorais / Publisher's copyright statement:

Holographic recording and characterization of photorefractive Bi$_2$TeO$_5$ crystals at 633 nm wavelength light

Ivan de Oliveira,[1,a)] Jesiel F. Carvalho,[2,b)] Zanine V. Fabris,[2] and Jaime Frejlich[3,c)]
[1]*Grupo de Óptica e Modelagem Numérica (GOMNI)-Faculdade de Tecnologia/UNICAMP, Limeira-SP, Brazil*
[2]*Instituto de Física/Universidade Federal de Goiás, Goiânia-GO, Brazil*
[3]*Instituto de Física "Gleb Wataghin"/UNICAMP, Campinas-SP, Brazil*

We report on the holographic recording on photorefractive Bi$_2$TeO$_5$ crystals using $\lambda = 633$ nm wavelength light. We studied the behavior of this material under the action of this low photonic energy light and found out the presence of a fast and a slow hologram, both of photorefractive nature and exhibiting rather high diffraction efficiencies. The faster and the slower holograms are based on the excitation and diffusion of oppositely charged carriers (likely electrons and holes). Relevant parameters for the photoactive centers responsible for both kind of holograms were characterized using purely holographic techniques. No evidences of non-photosensitive ionic charge carriers being involved in the recording process at room temperature nor self-fixing effects were found. © 2014 AIP Publishing LLC. [http://dx.doi.org/10.1063/1.4871807]

I. INTRODUCTION

Bismuth Tellurite Oxide Bi$_2$TeO$_5$, here labelled BTeO, is a photorefractive material that crystalizes in a non-centrosymmetric orthorhombic structure, with space group Abm2.[1] Its capability as medium for holographic recording has been already reported by other researchers,[2–6] that pointed out some of its useful properties: Rather transparent in the visible spectral range, long lifetime recorded holograms, good capabilities as data storage medium, and rather large diffraction efficiency. However, to our knowledge, holographic recording experiments were reported up to now, using lasers in the blue-green wavelength (475–532 nm) range only. In this work, we show, for the first time to our knowledge, that it is also possible to record efficient holograms in this material using light ($\lambda = 633$ nm) of lower photonic energy ($\approx$2 eV) and report the presence of a fast and a slow hologram that are both quantitatively characterized using purely holographic techniques.

II. CRYSTAL GROWING

The BTeO crystals were produced by a double crucible Czochralski method[7] at the Institute of Physics of the Federal University of Goiás, at Goiânia, Brasil. Crystal growth of BTeO presents some inherent difficulties because of (a) pronounced cleavage through the (100) crystallographic plane and (b) the high partial vapor pressure of tellurium oxide near the melting point. In order to minimize the latter effect, TeO$_2$-excess was used in the starting composition, as suggested elsewhere.[4] Bismuth oxide (Bi$_2$O$_3$, Sigma-Aldrich, 99 999%) and tellurium oxide (TeO$_2$, Sigma-Aldrich, 9999%) were mixed in the molar ratio of 1:1.1, being pre-synthesized by solid-state reaction before

melting in platinum crucibles. Crystal growth was done on seeds oriented along [001] direction, keeping the cleavage plane in the vertical to prevent cracking during growing. Crystal growth was performed in a resistive furnace with temperature stability better than 0.2 °C and axial temperature gradient above the melt of about 30 °C/cm, equipped with a pure platinum seed holder controlled by an accurate pulling and rotation system. All runs were carried out in air, and the best parameters were pulling rate of 0.3 mm/h and rotation rate of 15 rpm. The pulling and rotation rates were kept constant in each experiment during the entire process, and the crystal diameter was controlled by changing the furnace temperature. Figure 1 shows polished samples of BTeO crystals similar to those used in this work. Fig. 2 shows the optical transmittance spectrum curve in the 400–800 nm range, looking similar to that reported elsewhere[8] for this material, where absorption bands due to impurities or defects are not observed. White light pre-exposure reduces the transmittance in the 500–800 nm range. This may indicate the presence of empty localized photoactive centers at energies up to about 2.5 eV (corresponding to 500 nm wavelength) from the
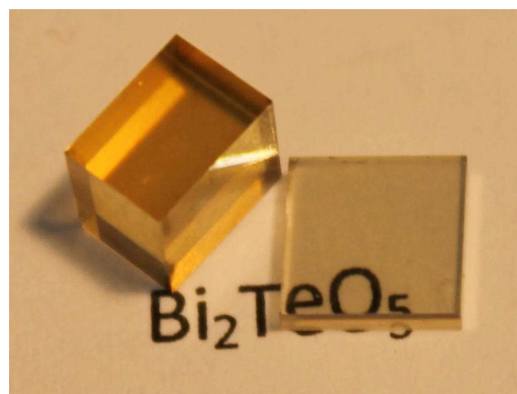

FIG. 1. Polished BTeO crystal samples produced at the Federal University of Goiás, Goiânia, Brazil.

a)Electronic mail: ivan@ft.unicamp.br
b)Electronic mail: carvalho@if.ufg.br
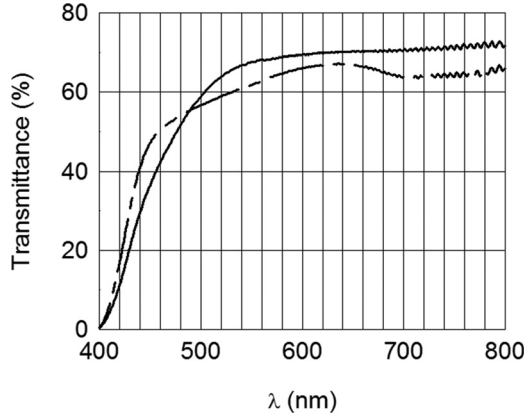c)Electronic mail: frejlich@ifi.unicamp.br

FIG. 2. Optical transmittance at room temperature for a thermally relaxed BTeO sample kept for 1 h at 300 °C (continuous curve) and (dashed curve) after several hours exposed to white light.

extended state, where charge carriers can be optically pumped to.

III. HOLOGRAPHIC RECORDING AND ERASING

Holograms were successfully recorded using direct $\lambda = 633$ nm as schematically illustrated in Fig. 3. The grating vector $\vec{K}$ ($K = 2\pi/\Delta$, Δ being the grating spatial period) is always parallel to the [010] crystal axis, and beams' polarization is always vertical and parallel to the [001] axis. From the characteristic gaussian shaped transverse laser light intensity distribution $I(r)$ (r being the radial beam coordinate) and total beam power expressions,

$$I(r) = I_0 e^{-r^2/R^2} R \approx 1.4\,\text{mm}\,, \qquad (1)$$

$$P = \int_0^{r=R} I(r) 2\pi r dr = \pi R^2 I_0, \qquad (2)$$

the maximum intensity $I_0 \propto P$ of the gaussian beams may be estimated. The recorded hologram is erased using one ($\mathbf{I}_S^0$) of the two recording beams while the other ($\mathbf{I}_R^0$) one is switched off. The maximum irradiance of the erasing beam, as computed from Eqs. (1) and (2), is the relevant parameter here as
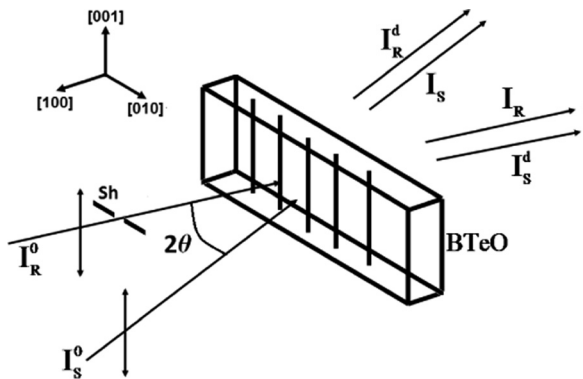

FIG. 3. Schematic illustration of the recording setup: BTeO is the crystal, $\mathbf{I}_S^0$ and $\mathbf{I}_R^0$ are the intensity of the two incident recording beams (referred to as "signal" and "reference," respectively), whereas $\mathbf{I}_S$ and $\mathbf{I}_R$ represent their intensity behind the crystal, with $\mathbf{I}_S^d$ being the diffracted signal beam. The shutter is **Sh** and $\mathbf{I}_S^0/\mathbf{I}_R^0 \approx 4.4$ throughout.

it determines the maximum diffraction efficiency and speed that are measured during erasure. The diffraction efficiency is computed as $\eta = \mathbf{I}_S^d/(\mathbf{I}_S^0 + \mathbf{I}_S^d)$ during erasure (that allows neglecting bulk light absorption because all intensities are measured behind the crystal) and plotted as a function of time.

For the case of rather low diffraction efficiency (Figures 7–9), curves were fitted using the in-Bragg diffraction efficiency (η) formulation for a purely phase photorefractive volume grating[10–12]

$$\eta = \sin^2(\kappa d), \qquad \kappa d \equiv \frac{\pi n^3 r_{\text{eff}} |E_{\text{sc}}(t)|}{2\lambda \cos\theta} d, \qquad (3)$$

$$E_{\text{sc}}(t) = A_F e^{-\Delta t/\tau_F} + e^{-i\varphi} A_S e^{-\Delta t/\tau_S}, \qquad (4)$$

where n is the refractive index, r_{eff} the effective electro-optic coefficient, $E_{\text{sc}}(t)$ the time-evolving space-charge electric field amplitude, $\lambda = 633$ nm the recording light wavelength, 2θ the angle between the incident recording beams inside de crystal, t_0 in $\Delta t \equiv t - t_0$ is the initial time for erasure, and A_F and A_S are the amplitudes of the fast and slow holograms, respectively, with φ representing the phase shift between them with their corresponding space-charge response times τ_F and τ_S that are formulated as[13]

$$\tau_F \approx \tau_F^{\text{sc}} = \tau_{MF} \frac{1 + K^2 L_{DF}^2}{1 + K^2 l_{sF}^2}, \qquad (5)$$

$$\tau_S = \frac{\tau_S^{\text{sc}}}{1 - \kappa_{12}\kappa_{21}} \qquad \tau_S^{\text{sc}} = \tau_{MS} \frac{1 + K^2 L_{DS}^2}{1 + K^2 l_{sS}^2}, \qquad (6)$$

with

$$1/\kappa_{12} = 1 + K^2 l_{sF}^2 \qquad 1/\kappa_{21} = 1 + K^2 l_{sS}^2, \qquad (7)$$

and

$$\tau_{Mj} = \frac{\epsilon\varepsilon_0}{q^2 L_{Dj}^2} \frac{h\nu}{\Phi_j I\alpha}, \qquad (8)$$

with $j = S, F$ and I being the irradiance, α the intensity exponential absorption coefficient, q the value of the charge of the electron, ε_0 the permittivity of vacuum, ϵ the dielectric constant, and Φ_j the quantum efficiency for photoexcitation from the fast ($j = F$) and the slow ($j = S$) photoactive centers, respectively. However, for higher diffraction efficiency where self-diffraction effects cannot be neglected[14] during erasure, as is the case in Fig. 4, the slow and the fast gratings were separately fitted using[9]

$$\eta = |J_0(\sqrt{i8\kappa dt/\tau_S})e^{-t/\tau_S}|^2, \qquad (9)$$

$$1 - \eta = |1 - J_0(\sqrt{i8\kappa dt/\tau_F})e^{-t/\tau_F}|^2, \qquad (10)$$

respectively, where J_0 is the zero order ordinary Bessel function. Equations (9) and (10) result from the fact that the reading beam is diffracted by the already recorded reversible grating thus producing a recording pattern of fringes that modifies the erasure process.
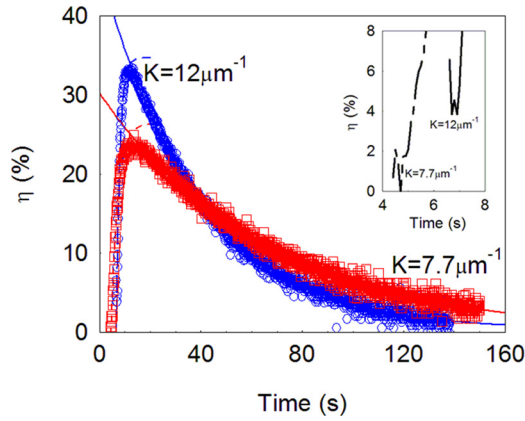
FIG. 4. Holograms recorded with $K = 12 \, \mu m^{-1}$ (°) and $K = 7.7 \, \mu m^{-1}$ (□) for 10 min with 11.7 mW (maximum irradiance $\approx$190 mW/cm²) total power beam and erased using I_S^0, showing a fast and a slow hologram that are mutually phase shifted by approximately $\varphi = \pi$. The continuous lines are the best fitting of the slow hologram with Eq. (9), and the dashed lines are the corresponding fitting of the fast holograms with Eq. (10). The inset shows an amplification of the initial part of the erasure for both curves. The resulting parameters are reported on Table I.

A. Slow and fast holograms

Holograms were recorded on a crystal sample of thickness $d = 2.6$ mm, and the erasure curves displayed in Fig. 4 show the typical features of the simultaneous presence of a fast and a slow mutually phase shifted gratings.[15] Both curves here (see inset figure) show a sharp decrease in overall diffraction efficiency (η) at the very erasure beginning (indicating the erasure of an initially larger fast grating) followed by an increasing η indicating the progressive disclosing of the almost unchanged slow (approximately counterphase) grating during the faster grating erasure; the maximum of this erasure curve occurs when the faster hologram is completely erased and, therefore, approximately represents the size of the slower grating. The best fitting parameters of data in Fig. 4 are reported in Table I. Curves in Fig. 4 qualitatively show that the slow and the fast gratings are roughly counterphase ($\varphi \approx \pi$), thus indicating that oppositely charged carriers are involved. We also see that the response times τ_F and τ_S do depend on K (see for example Ref. 16), thus indicating that a diffusion mechanism is involved as expected for a photorefractive recording process in agreement with Eqs. (5) and (6).

B. Slow hologram saturation

Recording on the same crystal sample, but with increasing recording time, was carried out in order to find out saturation conditions for the slower hologram. For this doing, the slow hologram amplitude was estimated, as discussed before, from the maximum of the erasure curve. Diffraction

TABLE I. Parameters from fitting of data in Fig. 4.

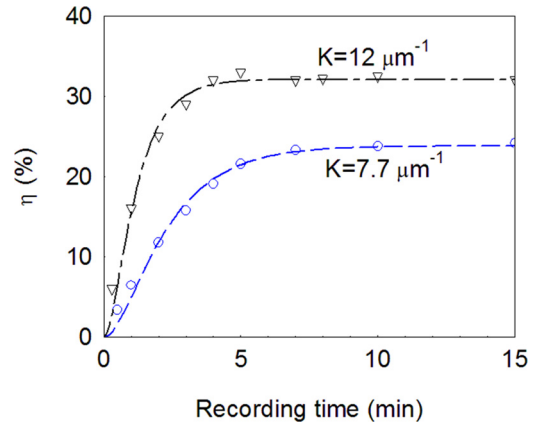| K (μm^{-1})	τ_F (s)	τ_S (s)
7.7	5.2 ± 0.2	335 ± 30
12	3.0 ± 0.4	249 ± 3

FIG. 5. Diffraction efficiency of the slow hologram as a function of the recording time, showing saturation being achieved at about 5 min with a maximum $\eta \approx 32\%$ for $K = 12 \, \mu m^{-1}$ and a somewhat lower value for $K = 7.7 \, \mu m^{-1}$. Dashed lines are just a guide for the eyes.

efficiencies obtained in this way were plotted in Fig. 5, showing that the time for slow hologram saturation is different for different hologram vector $\vec{K}$ values.

C. Light intensity dependence of Debye and diffusion lengths

Parameters τ_F and τ_S were computed from experimental data, as for the case of Fig. 4, but for varying K, and plotted in Fig. 6 for total recording beams power (in the air) $P \approx 11.7$ mW and in Fig. 7 for $P \approx 1$ mW. Parameters from curves fitting with Eqs. (5) and (6) in Figs. 6 and 7 are reported in Table II.

Note that there is no curve for the slow hologram for the low power case of Fig. 7, because the irradiance is not strong enough to allow recording such a hologram with good quality. Data in Table II do confirm recently reported[17] theoretical and experimental results (although for another photorefractive material) showing that the Debye length (l_s) should increase as the irradiance onto the crystal decreases. As there is also a relation between l_s and the diffusion length L_D,[18] the latter should also increase as l_s increases, as actually shown in Table II, also in agreement with recently published results.[19]
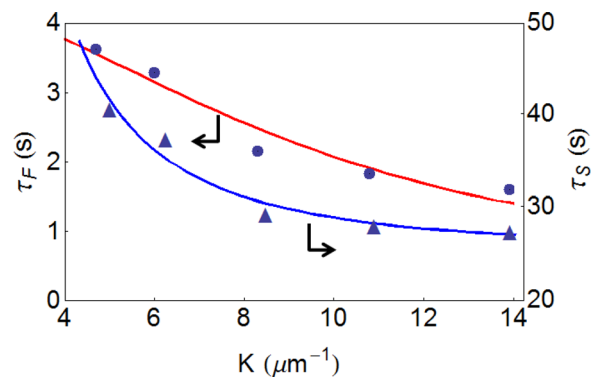

FIG. 6. Parameters τ_F and τ_S computed in conditions similar to those reported for Fig. 4, and plotted as a function of K, for total laser beams power $P \approx 11.7$ mW. Curves fitted to Eqs. (5) and (6) lead to the parameters reported in Table II.

TABLE II. Parameters from fitting of curves in Figs. 6 and 7.

P (mW)	L_{DF} (μm)	L_{DS} (μm)	l_{sF} (μm)	l_{sS} (μm)	τ_{MF} (s)	τ_{MS} (s)	Φ_F	Φ_S
1	0.88	…	0.13	…	…	…	0.2	…
11.7	0.02	0.26	0.05	0.34	4.4	44	0.2[a]	0.01

[a]Substituted from the previous line.

TABLE III. Parameters from fitting of curves in Fig. 8.

Recording time	τ_F (s)	τ_S (s)	φ (rad)
50	2.0	…	…
120	3.2	3000	4.3
300	3.2	3200	4.3

Holograms were also recorded and erased, as described above, on a slightly thinner (2.2 mm thick) sample from the same crystal boule but with a larger input surface plane so as recording could be restricted to the center of the sample with minimum parasitic scattering from its borders, thus facilitating measurement of holograms with reduced η. The latter were in fact recorded using lower (50, 120, and 300 s) recording time, for $K = 4.4$ μm^{-1}, and displayed in Fig. 8. In this case, as $\eta \ll 1$, the latter can be approximately represented by the diffracted intensity $\mathbf{I}_S^d$. Curves here were fitted using Eq. (3), and resulting parameters are reported on Table III.

Table III and Fig. 8 show that, as the recording time increases, also increases the amplitude of the slow hologram A_S, as should be expected if we are not close to saturation. The first row in Table III, showing a very different value for τ_F and lacking information about the slow grating, is just reported in order to put into evidence our experimental limitations for low recording time. As a consequence, note that it is not $\varphi \approx \pi$ in Table III, different than deduced from Fig. 4, probably because the relatively low recording time here did not allow for good stabilization conditions for recording.

D. Photorefractive nature of the recording process

The expressions in Eqs. (5)–(8) explicitly state that the recording time does depend on the spatial grating period (because of charge carriers diffusion) as well as on the recording light irradiance (because of the excitation of charge carriers by photons). Both these conditions are the main characteristics of a photorefractive based process. The former dependence has been already demonstrated from data in Table I and more precisely from the good data fitting in Figs.
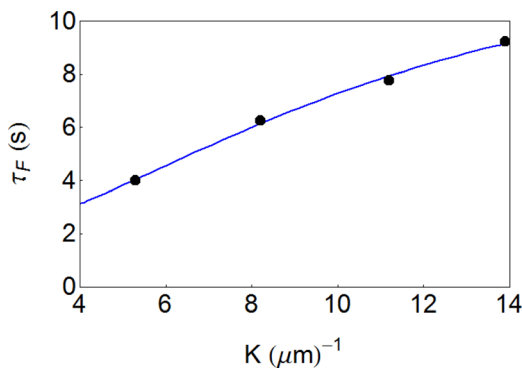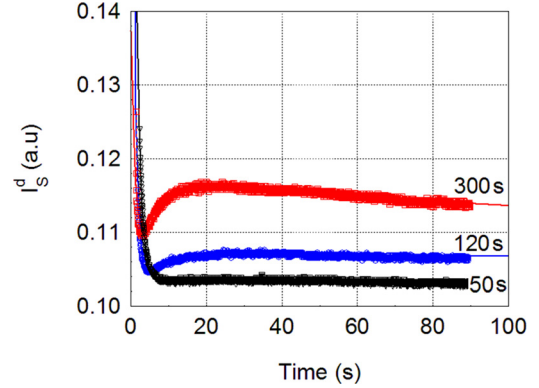

FIG. 8. Diffracted intensity $\mathbf{I}_S^d \propto \eta$ (in arbitrary units, with $\eta \ll 1$) during erasure of holograms recorded (11.7 mW total beams power) on a larger surface and slightly thinner (2.2 mm thick) crystal sample, with $K = 4.4\,\mu$m^{-1}.

6 and 7. It is, nevertheless, important to realize that the recording time may decrease (see Fig. 7) or increase (see Fig. 6) with K depending upon the relative weight of terms $K^2L_D^2$ and $K^2l_s^2$ in Eqs. (5) and (6), and that these terms also depend, via L_D and l_s, on the irradiance I. The light intensity dependence is still to be proved on a quantitative basis. For this doing, we recorded and erased holograms in the 2.6 mm thick sample with two wide different laser beam power (all other experimental conditions remaining as before for this sample) and computed the corresponding response time from erasure curves fitting, following the same procedure reported above. Results are shown in Fig. 9, and the parameters from curves fitting are reported in Table IV.
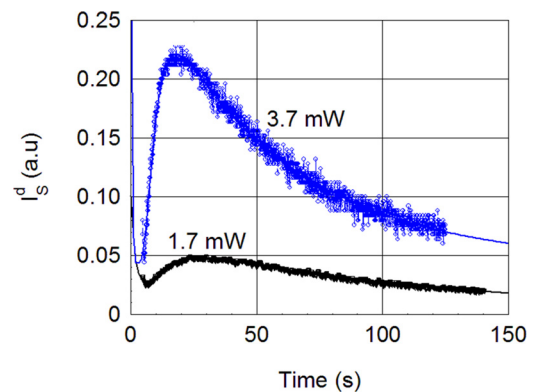

FIG. 7. Parameters τ_F, for total laser beams power $P \approx 1$ mW, were computed as for those in Fig. 4, but fitting to Eq. (3) where self diffraction is neglected due to the lower diffraction efficiency here. As for Fig. 6, τ_F was plotted as a function of K and fitted to Eq. (5) leading to the parameters reported in Table II.

FIG. 9. Diffracted intensity $\mathbf{I}_S^d \propto \eta$ (in arbitrary units, with $\eta \ll 1$) during erasure of fast and slow holograms, recorded in the 2.6 mm thick sample, for 3 min, with total laser power beams of 1.7 mW and 3.4 mW, with $K = 11.2\,\mu$m^{-1}. Parameters computed from fitting with Eq. (3) are reported in Table IV.

TABLE IV. Parameters from curves in Fig. 9.

Total power (mW)	P^{a}	τ_F (s)	τ_S (s)	$\tau_F \times P$ (mJ)	$\tau_S \times P$ (mJ)
1.7	1.4	7.8	183	10.9	256
3.4	2.8	3.8	107	10.6	300

[a] P: Erasing (signal) beam power.

The latter table clearly shows that both τ_S and τ_F decrease as the power P of the erasing beam increases. In fact, for the rather low P in this experiment, the corresponding L_D[19] and l_s[17] parameters in Eqs. (5) and (6) are approximately independent from P, and it is therefore possible to verify that the power × response-time ($P \times \tau_{F,S}$) product is constant within 3% limit for the faster hologram and within 12% limit for the slower one. The clearly established inverse dependence of τ_S and τ_F on the light irradiance, together with their previously demonstrated dependence on K, are definite evidences of the photorefractive nature of the present recording process.

IV. CONCLUSIONS

We have shown that it is possible to record rather efficient photorefractive holograms in BTeO not only in the blue-green spectral range as already reported in the literature but also using less energetic 633 nm wavelength red light. At least for this light, a fast and a slow hologram were recorded that are based on the movement of oppositely charged carriers, probably electrons and holes. The diffusion and Debye lengths were estimated for both holograms, which values were shown to depend on the light irradiance, in agreement with previously reported results but for other photorefractive materials.

The presently observed behavior of Bi_2TeO_5 under red light may probably occur in a wider wavelength spectral range too, and should be investigated and taken into account for technical applications using this material. Different than reported elsewhere,[20] we did not detect sensible participation of ionic charge carriers in the recording process neither associated self-fixing effects in this material, at least at room temperature.

[1] D. Mercurio, M. El Farissi, B. Frit, and P. Goursat, "Etude structurale et densification d'un nouveau materiau piezoelectrique: Bi₂TeO₅," Mater. Chem. Phys. **9**, 467–476 (1983).
[2] I. Földvári, M. P. Scripsick, L. E. Halliburton, and A. Péter, "Photorefractive effects in Bi₂TeO₅ single crystals," Phys. Lett. A **154**, 84–86 (1991).
[3] I. Földvári, H. Liu, and R. Powell, "Investigation of the photorefractive effect in Bi₂TeO₅," J. Appl. Phys. **71**, 5465–5473 (1992).
[4] I. Földvári, A. Péter, O. Szakács, A. Munoz, and F. Visinka, "Improvement in quality and performance of photorefractive Bi₂TeO₅," J. Crys. Growth **198/199**, 482–486 (1999).
[5] I. Földvári, C. Denz, A. Péter, J. Petter, and F. Visinka, "Bismuth tellurite—a new material for holographic memory," Opt. Commun. **177**, 105–109 (2000).
[6] W. Horn, I. Földvári, and C. Denz, "Holographic data storage in photorefractive bismuth tellurite," J. Phys. D: Appl. Phys. **41**, 224006 (2008).
[7] J. F. Carvalho, Z. V. Fabris, I. de Oliveira, and J. FrejlichI, "Crystal growth of Bi₂TeO₅ by a double crucible czochralski method," J. Cryst. Growth (in press).
[8] I. Földvári, A. Péter, R. Voszka, and L. A. Kappers, "Growth and properties of Bi₂TeO₅ single crystals," J. Cryst. Growth **100**, 75–77 (1990).
[9] I. de Oliveira and J. Frejlich, "Gain and stability in photorefractive two-wave mixing," Phys. Rev. A **64**, 033806 (2001).
[10] H. Kogelnik, "Coupled wave theory for thick hologram gratings," Bell Syst. Tech. J. **48**, 2909–2947 (1969).
[11] L. Solymar and J. Cooke, *Volume Holography and Volume Gratings* (Academic Press, London, New York, Toronto, Sydney, San Francisco, 1981).
[12] J. Frejlich, *Photorefractive Materials: Fundamental Concepts, Holographic Recording, and Materials Characterization* (Wiley-Interscience, New York, 2006), Chap. IV.
[13] R. Montenegro, A. Shumelyuk, R. Kumamoto, J. F. Carvalho, R. C. Santana, and J. Frejlich, "Vanadium-doped photorefractive titanosillenite crystal," Appl. Phys. B **95**, 475–482 (2009).
[14] F. Horowitz, D. Kligler, and B. Fisher, "Time-dependent behavior of photorefractive two- and four-wave mixing," J. Opt. Soc. Am. B **8**, 2204–2217 (1991).
[15] S. Zhivkova and M. Miteva, "Holographic recording in photorefractive crystals with simultaneous electron-hole transport and two active centers," J. Appl. Phys. **68**, 3099–3103 (1990).
[16] N. Korneev, D. Mayorga, S. Stepanov, A. Gerwens, K. Buse, and E. Krätzig, "Characterization of photorefractive strontium-barium niobate with non-steady-state holographic photocurrents," Opt. Commun. **146**, 215–219 (1998).
[17] I. de Oliveira and J. Frejlich, "Light intensity dependent Debye screening length in undoped photorefractive titanosillenite crystals," J. Appl. Phys. **112**, 113523 (2012).
[18] J. Frejlich, *Photorefractive Materials: Fundamental Concepts, Holographic Recording, and Materials Characterization* (Wiley-Interscience, New York, 2006), Appendix D.
[19] I. de Oliveira, J. F. Carvalho, and J. Frejlich "Resonance running hologram velocity nonlinearity dependence upon light intensity in photorefractive crystals," Appl. Phys. Lett. **102**, 251913 (2013).
[20] G. Berger, C. Denz, I. Foldvari, and A. Peter, "Non-volatile volume holograms in bismuth tellurite crystals," J. Opt. A: Pure Appl. Opt. **5**, S444–S447 (2003).